Full Paper

Static and Dynamic Permittivity Measurement of High Explosives in the W Band to Investigate Shock and Detonation Phenomena

Benoit Rougier,*[a, b] Alexandre Lefrançois,[a] Vincent Chuzeville,[a] Sandra Poeuf,[a, c] and Hervé Aubert[b]

Abstract: Radio interferometry techniques are often used to investigate shock and detonation phenomena thanks to the radio-transparency of high explosives in the gigahertz frequency band. These techniques require the knowledge of the permittivity of studied explosives. Although the permittivity has been thoroughly studied for many materials, very few data are available at high frequencies (>75 GHz) for high explosives. In this paper, we report static measurement data of the permittivity for various reactive materials using the standard *line transmission method* between 75 GHz and 110 GHz (W frequency Band), and we present dynamic measurement results at 94 GHz obtained from the so-called *detonation wavefront tracking method*. It is shown that the measurement results provided by these two methods are in good agreement. As a consequence, this work validates the detonation wavefront tracking method for the dynamic measurement of high explosives permittivity, and shows that the static experimental results are relevant for shock wave propagation analysis from millimeter-wave measurement techniques.

Keywords: High explosive · detonation velocity · measurement of relative permittivity · millimeter-wave

1 Introduction

The dielectric properties of high explosives are a key indicator in several applications such as understanding microwave heating and ignition [1] or explosive detection for safety purposes [2,3] in the various frequency bands, including [60–90] GHz. Another application is the characterization of detonation properties [4] where the parameter of interest is the detonation velocity. Several techniques exist for measuring this key indicator, such as, electronic pins [5], Fiber Bragg Grating systems [6] or Radio-InterFerometry (RIF) [7]. The RIF techniques require the knowledge of the dielectric constant (or real part of the relative dielectric permittivity) of the sample under study, for which several static methods exist, such as, e.g., open-ended coaxial probe techniques, transmission line methods, resonant cavity set-up [8] or reflectivity-based methods [9]. These techniques have been successfully applied to the characterization of high explosives, but very few measurement data are available in the millimeter-wave frequency range. In this frequency range, most high explosives are transparent and therefore can be advantageously analyzed using RIF techniques. Cawsey et al. [10] studied high explosives at 34.5 GHz for various densities by applying the resonant cavity method. Daily et al. [11] derived the dielectric constant of thirteen reactive materials in the 8–12 GHz frequency range with the circular cavity technique. Higginbotham Duque et al. [12] developed a cavity perturbation method to analyze nine materials based on TATB, RDX and HMX from 1 to 18 GHz. Glover and Perry [13] studied TATB using the scattering matrix in the same frequency range, while Smith et al. [2] used space reflection methods to measure the dielectric properties of P1000.

Another standard technique for measuring the dielectric constant of high explosives materials consists in tracking the detonation wavefront of a bare cylinder. Tringe et al. [14] implemented this method to analyze the properties of LX-10. The results were compared with static measurement data by using a coaxial probe on three HMX-based compositions. They were in good agreement within 6% (which results in 3% difference between the detonation velocities), even though the densities of materials differed and comparisons were not performed at same frequencies.

In this paper, we present dynamic measurements of the bare cylinder complex permittivity using the detonation wavefront tracking method, as well as static measurement obtained from the standard transmission line method. The

[a] B. Rougier, A. Lefrançois, Dr. V. Chuzeville, S. Poeuf
CEA, DAM, CEA Gramat
F-46500, Gramat, France
*e-mail: brougier@laas.fr
[b] B. Rougier, Prof. H. Aubert
LAAS CNRS, Toulouse University, CNRS, INPT
7 Avenue du Colonel Roche, 31077, Toulouse, France
[c] S. Poeuf
Institut P', UPR CNRS 3346, ENSMA, Université de Poitiers
86961, Futuroscope-Chasseneuil Cedex, France

Full Paper

B. Rougier, A. Lefrançois, V. Chuzeville, S. Poeuf, H. Aubert
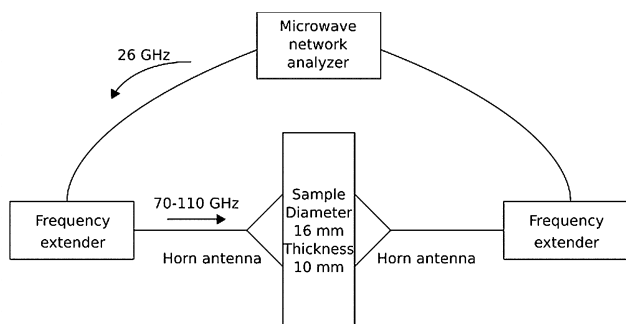

Figure 1. Schema of the experimental setup for static measurement of reactive material complex permittivity in the W frequency band (transmission line method).

results obtained from static and dynamic measurements are compared for the same material and at the same frequency. A special attention is focused on the measurement uncertainty of the complex permittivity associated with the two measurement techniques.

2 The Transmission Line Method in the W-Band

Firstly, to measure the permittivity of reactive materials, the transmission line method is applied. A microwave network analyzer N5260A from Agilent Technologies generates a microwave signal at about 26.5 GHz, whose frequency is increased by using the V10VNA2-T/R frequency extension module from Agilent Technologies. The resulting frequency is in the W range, that is, between 75 GHz and 110 GHz. Next, this signal is transmitted into a material under test. This material is cylindrical with a diameter of 16 mm and is 10 mm thick. It is placed between two dedicated rectangular horn antennas. A schema of the setup is presented in Figure 1.

As the loss tangent of reactive materials is particularly low, a modified Nicholson Ross Weir (NRW) method [15,16] is applied here to determine the relative permittivity of the sample. From the measured scattering matrix $[S_{i,j}]$ ($i = 1, 2$ and $j = 1, 2$), the reflection Γ and transmission T coefficients are derived as follows [15,16]:

$$\Gamma = \frac{S_{11}^2 - S_{21}^2 + 1}{2S_{11}} \pm \sqrt{\left(\frac{S_{11}^2 - S_{21}^2 + 1}{2S_{11}}\right)^2 - 1}, \quad (1)$$

$$T = \frac{S_{11} + S_{21} - \Gamma}{1 - (S_{11} + S_{21})\Gamma}. \quad (2)$$

The dielectric constant $\mathrm{Re}(\varepsilon_r)$ and imaginary part $\mathrm{Im}(\varepsilon_r)$ of the complex relative permittivity ε_r are then computed from the following relationships:

$$\mathrm{Re}(\varepsilon_r) = \left(\frac{c_0 \alpha}{2\pi df}\right)^2, \quad (3)$$

$$\mathrm{Im}(\varepsilon_r) = -\frac{c_0 \ln(|T|)\sqrt{\mathrm{Re}(\varepsilon_r)}}{\pi df}. \quad (4)$$

where α is the phase of transmission coefficient T, d is the thickness of the sample, f is the operating frequency and c_0 is the speed of light in vacuum.

Two main uncertainties may impact the estimation accuracy of the permittivity: (1) the uncertainty on the sample thickness (± 0.1 mm), and (2) the uncertainty on the position of the sample in the holder (not determined here). Additionally, the machining error can lead to the non-parallelism of the opposite sides of the sample and therefore, may result in the non-optimal contact between the sample and the two horn antennas. In order to analyze the impact of eventual mechanical imperfections on the measurement results, two series of measurement are performed for each material, and allow checking the reproducibility and reliability of measurement results. To compute the uncertainty, the mean of each series of measurement is taken. The samples were controlled in thickness, giving an uncertainty on this parameter. With eqs. (3) and (4), an uncertainty on each mean of a series was computed. The final value is the mean of all series for a sample, the uncertainty has been computed using propagation method.

As a very first experimental validation, the dielectric constant $\mathrm{Re}(\varepsilon_r)$ of the Teflon is measured. Two sets of ten measurements are performed. The scattering matrix is measured with a frequency step of 400 MHz. For each frequency, the average between the two set of measurements is computed. The average deviation between the two sets of measurements is of 0.1 for the dielectric constant and 0.02 for the imaginary part $\mathrm{Im}(\varepsilon_r)$. The obtained real and imaginary parts of the relative permittivity ε_r are reported as a function of frequency in Figure 2 and Figure 3, respectively. At 94 GHz, the real $\mathrm{Re}(\varepsilon_r)$ and imaginary $\mathrm{Im}(\varepsilon_r)$ parts of the complex dielectric constant ε_r are computed from the averaging between 93 GHz and 95 GHz (see Figures 2 and 3). The resulting permittivity ε_r at this frequency is $1.96 - 0.06j$. The measurement uncertainty with a normal law at $k = 2$ is of 0.237 for the real part and 0.061 for the imaginary part. These values are consistent with the reported data [17] (the difference is of 4.7%). The mass density of the sample under test is 2144 kg m^{-3}.

Next, fourteen energetic materials of two different types, non-aluminized and aluminized materials, were tested. They are fabricated by using the three main processing methods: cast-cured, pressed and melted high explosives. The compositions of each sample are given in Table 1 and the results are reported in Table 2.
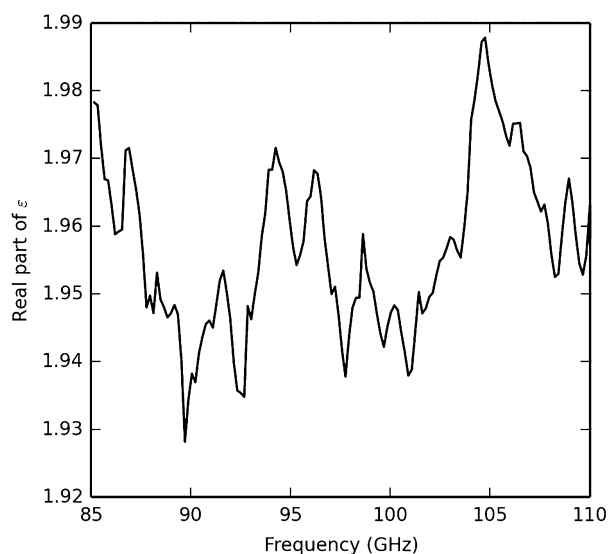
Static and Dynamic Permittivity Measurement of High Explosives in the W Band to Investigate Shock and Detonation Phenomena

**Propellants,
Explosives,
Pyrotechnics**

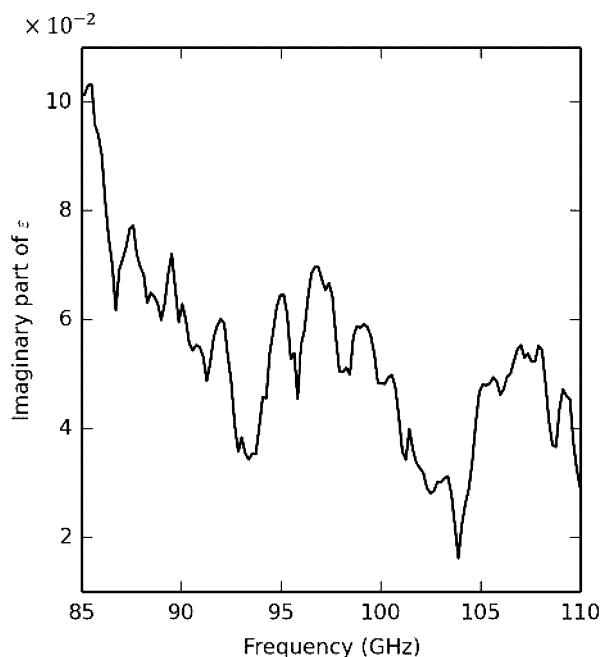**Figure 2.** Dielectric constant of Teflon as a function of frequency.

Figure 3. Imaginary part of the relative permittivity of Teflon as a function of frequency.

3 The Detonation Wavefront Tracking Method (DFTM)

The determination of the relative permittivity by the bare cylinder test has already been reported [14]. It consists of monitoring the detonation velocity in the bare cylinder by using shorting pins and the millimeter-wave (94 GHz) interferometry technique. Shorting pins are placed along the cartridge to obtain a time-distance diagram, from which the

velocity V_{pins} is estimated by using the linear fitting of standard deviation δV_{pins}. Typically, two series of ten shorting pins were positioned on each side of the tested cylinder and curvature pins were placed at the back side. The detonation wavefront position is also recorded from a millimeter-wave interferometer operating at $f_c = 94$ GHz. The derivation of the velocity from the interferogram requires the knowledge of the material relative permittivity. The technique consists of equalizing the velocity obtained from the two methods by adjusting the value of the relative permittivity. The interferometer is composed of a millimeter-wave source, a Teflon waveguide of 5 m in length and a dielectric applicator which is stuck on the bare cylinder. The source generates an electromagnetic field in the applicator through a dielectric waveguide. The applicator is a dielectric cone of 16 mm in diameter and 80 mm in length. It allows transmitting the incident millimeter-wave and receiving the signal reflected by the sample under test. The experimental setup is sketched in Figure 4.

Once transmitted into the material, the incident electromagnetic wave is reflected by the detonation wavefront. This signal is then mixed with the incident wave in the interferometer to obtain the baseband signal. This signal is composed of two components which are in phase-quadrature. A typical signal for the detonation of sample 10 is shown in Figure 5. Two methods are implemented and compared for the processing of the reflected millimeter-wave signal.

In the first method, the displacement versus time obtained from the millimeter-wave interrogation is derived from the Lissajous method [18] with an initial arbitrary dielectric constant $Re(\varepsilon_{arb})$ in order to determine the pins velocity. The time derivative of this displacement yields to the velocity V_{arb}. As $\sqrt{Re(\varepsilon_r)}V$ is constant [7], the dielectric constant is then given by equation (5).

$$Re(\varepsilon_r) = Re(\varepsilon_{arb})\left(\frac{V_{arb}}{V_{pins}}\right)^2 \qquad (5)$$

The estimation accuracy of the dielectric constant is then related to the measurement uncertainty on V_{pins}.

The second method is based on the measurement of the Doppler frequency shift. The Fast Fourier Transform (FFT) is applied to the received signal to estimate the fre-
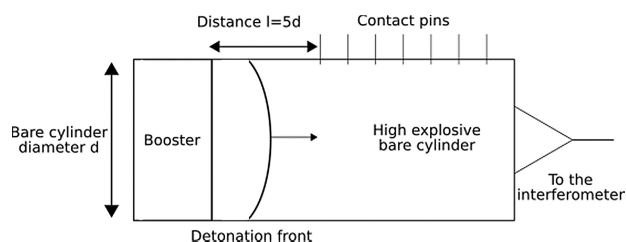

Figure 4. Sketch of the dynamic measurement setup (Detonation wavefront tracking method).

Table 1. Samples composition.

Family	Sample	Composition [wt%]	Nature	Density [g cm^{-3}]
TNT Group	S1	TNT (100)	Melt-cast	1.60
	S2[a]	RDX-TNT-wax (59.5/39.5/1)	Melt-cast	1.70
	S3[a]	RDX-TNT-wax (59.5/39.5/1)	Melt-cast	1.73
	S4[b]	NTO-TNT-wax (59.5/39.5/1)	Melt-cast	1.76
	S5[b]	NTO-TNT-wax (59.5/39.5/1)	Melt-cast	1.76
HMX Group	S6	HMX-NTO-inert binder (12/72/16)	Cast-cured	1.64
	S7	HMX-Aluminum- inert binder (45/35/20)	Cast-cured	1.73
	S8[c]	HMX inert- binder (96/4)	Pressed	1.47
	S9[c]	HMX- inert binder (96/4)	Pressed	1.86
RDX Group	S10	RDX- inert binder (85/15)	Cast-cured	1.58
	S11	RDX-NTO-Aluminum- inert binder (15/52/20/13)	Cast-cured	1.76
	S12	RDX-Aluminum inert -binder (64/20/16)	Cast-cured	1.65
TATB Group	S13	TATB- inert binder (97/3)	Pressed	1.88
	S14	TATB-HMX- inert binder (52/45/3)	Pressed	1.88

[a] Sample 2 and 3 have the same formulation but a different RDX is used: RS RDX Class III is used for the sample 6 and RDX CH and RDX B are used for the sample 3.
[b] Sample 4 and 5 have the same formulation but the NTO used comes from different manufacturers.
[c] Samples S8 and S9 are of the same composition, the only difference is the density.

quency f_D associated to the velocity of the detonation wavefront. The dielectric constant is then derived from equation (6). Two main uncertainties may impact the estimation accuracy of the permittivity: the resolution of the FFT, which is related to the measurement time, and the measurement uncertainty on V_{pins}. The typical spectrogram of the received signal for the TNT bare cylinder test is shown in Figure 6. The highest voltage peak is assumed to be the fundamental frequency, while the second and third peaks are harmonics.

$$Re(\varepsilon_r) = \left(\frac{c_0 \cdot f_D}{2 \cdot V_{pins} \cdot f_c}\right)^2 \tag{6}$$

The velocity derived from the shorting pins is computed with the time-position diagram. Note that the pins are placed at a distance of at least five diameters from the ignition point of the bare cylinder to measure a steady detonation wavefront. Moreover, as the detonation is ignited with a RP80 detonator and a HMX-based booster, the velocity measured at the beginning of the experiment might include the contribution of the booster. Since (1) the applicator of the interferometer is placed at the center of the cylinder and (2) the pins are located on the side, the time synchronization is performed taking into account the curvature of the detonation wavefront. This curvature is measured using curvature pins. The measured time-shift is typically about a few hundred nanoseconds. A comparison between the data giving by the shorting pins and those obtained from the millimeter-wave interrogation technique is reported in Figure 7. The uncertainty from the phase approach are computed using the known uncertainty on the position of the shorting pins and propagating this error. The uncertainty on the frequency approach is obtained with the uncertainty on the frequency measured with the FFT algorithm.

Table 2. Relative permittivity of various energetic materials at 94 GHz derived from the transmission line method (static measurement) and from the detonation wavefront tracking method (dynamic measurement).

Sample	Static direct measurement		Detonation wavefront tracking method	
	Real part of ε_r	Imaginary part of ε_r	Phase approach	Frequency approach
S1	2.87 ± 0.07	0.05 ± 0.02	2.787 ± 0.009	2.943 ± 0.057
S2	3.19 ± 0.07	0.07 ± 0.01	3.226 ± 0.031	3.227 ± 0.072
S3	3.32 ± 0.05	0.07 ± 0.01	3.274 ± 0.006	3.260 ± 0.074
S4	3.12 ± 0.07	0.07 ± 0.01	3.173 ± 0.004	3.181 ± 0.045
S5	3.13 ± 0.07	0.07 ± 0.01	3.173 ± 0.005	3.188 ± 0.051
S6	3.06 ± 0.06	0.08 ± 0.01	3.062 ± 0.010	3.126 ± 0.085
S7	5.73 ± 0.04	0.37 ± 0.11	–	–
S8	2.74 ± 0.06	0.06 ± 0.02	2.702 ± 0.005	2.687 ± 0.031
S9	3.43 ± 0.05	0.06 ± 0.02	3.409 ± 0.002	3.382 ± 0.061
S10	3.18 ± 0.05	0.09 ± 0.02	3.184 ± 0.010	3.158 ± 0.84
S11	4.52 ± 0.05	0.23 ± 0.02	–	–
S12	4.56 ± 0.12	0.20 ± 0.03	–	–
S13	4.42 ± 0.066	0.06 ± 0.01	4.462 ± 0.013	4.401 ± 0.040
S14	3.98 ± 0.06	0.05 ± 0.01	–	–

4 Analysis of the Measurement Results and Techniques

The measured complex permittivities of various energetic materials obtained from the transmission line technique

Static and Dynamic Permittivity Measurement of High Explosives in the W Band to Investigate Shock and Detonation Phenomena

**Propellants,
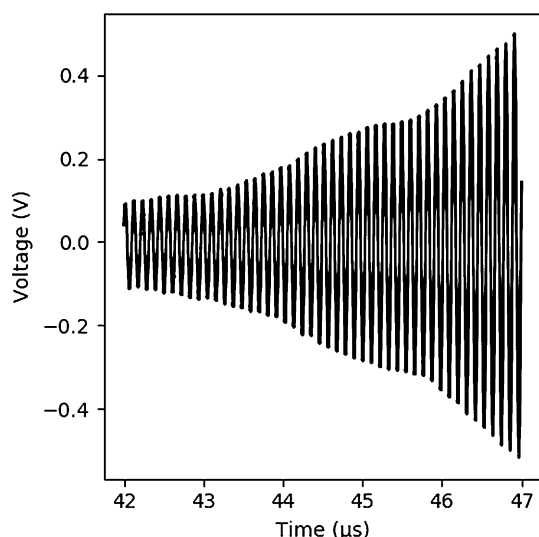Explosives,
Pyrotechnics**

Figure 5. Voltage signal received by the radio interferometer for the bare cylinder test of sample 10.
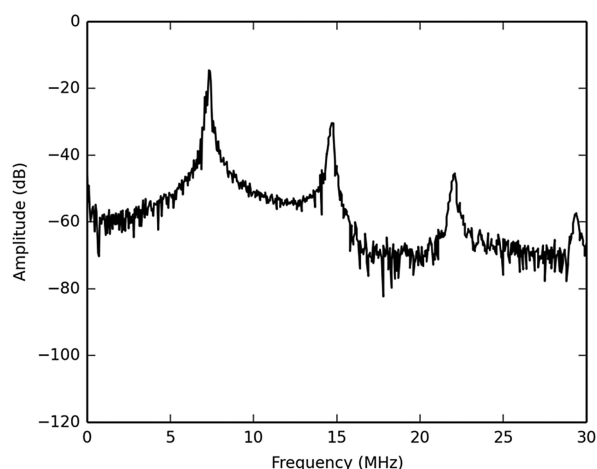
Figure 6. Spectrogram of the received signal for the TNT bare cylinder test.

Figure 7. Positions derived from shorting pins (stars and triangles) and from the millimeter-wave setup for sample 2 (line).

(static measurement) and from the detonation wavefront tracking technique (dynamic measurement) are reported in Table 2. Up to now, the detonation wavefront tracking method has not been applied to samples 7, 11, 12 and 14. The measurement uncertainty (assuming a normal law with $k = 2$) is lower than 0.072 for the dielectric constant (excepted for the aluminized compositions) and does not exceed 0.025 for the imaginary part of the relative permittivity. The estimation accuracy is degraded when samples include aluminum. The measurement errors are computed as the sum of errors on repeatability and reproducibility. Typically, the standard deviation for the shorting pins velocity is about 15 m s^{-1}, and the measurement time for the frequency-based method is around 12 µs, leading to sub-kilohertz resolution for the FFT. The largest uncertainties are of

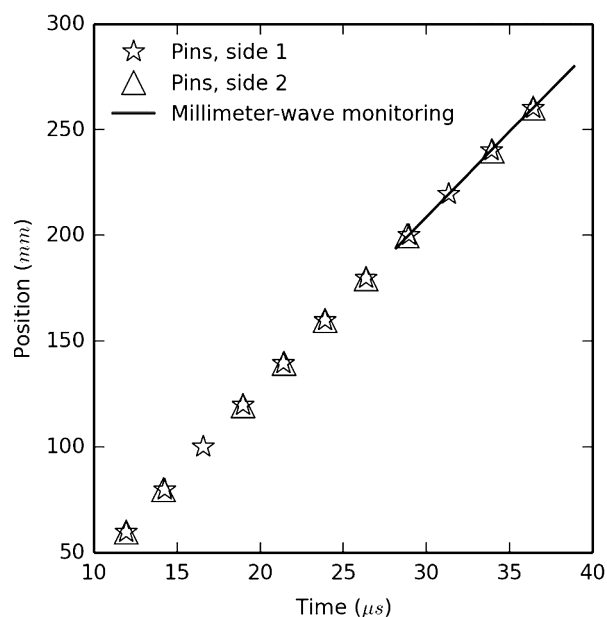0.031 and 0.085 for the quadrature and Doppler shift approaches. The dynamic measurement with the phase method provides the lowest standard deviation. The measured real part of the permittivity (or dielectric constant) given by the static method and that obtained from the DFTM are very close (the difference does not exceed 2%), excepted for the TNT sample for which the difference is around 2.7%. For the DFTM in phase and in frequency, the difference between the measurement results given by these two techniques are lower than 2%, excepted for the TNT sample, for which this difference is of 5.3%. This may be due to the poor quality of the bare cylinder assembly: a void has been identified at the interface between two blocks. Moreover, due to the uncertainties of the FFT, the uncertainty on the relative permittivity is higher when the frequency-based technique is applied. Losses in TNT have been reported in Ref. [11] at microwave frequencies (10 GHz). The losses reported here are ten times larger, but the operating frequency is much higher (94 GHz). It can be observed that the relative permittivity of aluminized high explosives (samples 7, 11 and 12) have been successfully measured, and tends to be higher (for both real and imaginary parts) than the permittivity of non-aluminized samples. This result has been obtained for various inert materials with metallic inclusions [19]. Here, samples 10 and 12 have similar compositions. In sample 12, the volume fraction of aluminum is of 12%, the variation of relative permittivity compared with the non-aluminized material is 44.4%. Compared to theoretical models and assuming inclusion of spherical particles, the Bruggeman formula (see eq.(7)) models correctly the addition of aluminum in sample 10 [20], where **Re**(ε_1) denotes the dielectric constant of the host material (here **Re**$(\varepsilon_1) = 10$) and
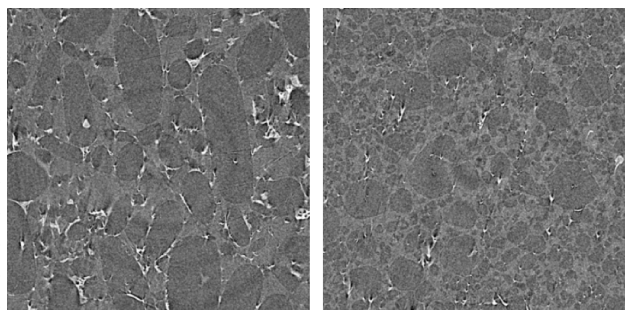
Figure 8. Microtomographies of samples 2 (left) and 3 (right), approximatively 3.2×3.2 mm^2.

$\mathbf{v}_2$ is the volume fraction of the inclusion (here the aluminum powder). According to this approach, the dielectric constant of sample 12 is 4.67. The difference with the measured dielectric constant is 1.6 %.

$$\mathbf{Re}(\varepsilon_{\mathbf{mix}}) = \frac{\mathbf{Re}(\varepsilon_1)}{(1 - \mathbf{v}_2)^3} \qquad (7)$$

As it can be observed from measurement results on samples 8 and 9, the dielectric constant changes when the mass density of the materials varies: the density difference is about 23 % and the variation of the dielectric constant is around 20 % for both measurement techniques. This result is consistent with the Landau Lifschitz Looyenga model [21] (see eq. (8)) that yields the value of 2.76 for the dielectric constant of sample 8 with a deviation of 0.68 % from the measurement. For samples 2 and 3, this model is still the most adequate. However, the deviation is larger (1.96 %).

$$\mathrm{Re}(\varepsilon_{\mathrm{mix}})^{\frac{1}{3}} = v_1 (\mathrm{Re}(\varepsilon_1))^{\frac{1}{3}} + v_2 (\mathrm{Re}(\varepsilon_2))^{\frac{1}{3}} \qquad (8)$$

The difference between the dielectric constants of samples 2 and 3 is of 4.17 % for the static measurement and around 1.50 % with using the DFTM. The difference is smaller with the DFTM because this method is based on the detonation velocity measurement. This velocity depends on the mass density of the samples, which differs slightly from one sample to another. The difference of composition (and therefore of the morphology of the grains) is expected to not change the detonation velocity, but to impact the static measurement results as suggested in Ref. [22]. As a matter of fact, Figure 8 shows the microtomographies of samples 2 and 3. It can be observed that grains of sample 2 are larger and more elliptic than those of sample 3. For sample 2, two main grain sizes are observed: 400 μm and 100 μm. For sample 3, some large grains, approximately 2 mm, are observed. The Landau Lifschitz Looyenga model is adequate but the deviation is around 2 % which could indicate that the grain morphology impacts the relative permittivity. On the opposite, the samples 4 and 5 (which are of the same composition, the same mass density and the same morphology of grains but are fabricated by two different NTO manufacturer), the difference does not exceed 0.3 %.

Table 3 reports the detonation velocities measured with shorting pins and from the phase analysis (static measurement of the relative permittivity ε_s). The measurement uncertainties are computed with the partial derivative method [23]. The difference between the two velocities is lower than 1 %, except for the TNT sample and the HMX-ONTA-inert binder sample (< 1.6 %). This comparison shows that the static and dynamic measurements are in very good agreement. All the measured data are reported in the supplementary information.

5 Conclusions

In this paper, the measurement of the dielectric constant of fourteen different high explosives, including aluminized HE, is reported. Two measurement techniques are applied: (1) a static approach based on the scattering matrix obtained

Table 3. Differences between the measured values of the dielectric constant and associated errors on the detonation wavefront velocity.

Sample	Detonation velocity with pins [m s^{-1}]	Detonation velocity from RIF measurements with static measurement of ε_r [m s^{-1}]	Difference [%] with the shorting pins as reference
S1	6697 ± 19	6589 ± 20	1.62
S2	7971 ± 44	8019 ± 87	0.60
S3	8133 ± 8	8076 ± 57	0.71
S5	7534 ± 6	7583 ± 87	0.65
S4	7480 ± 5	7543 ± 83	0.84
S6	7479 ± 20	7563 ± 68	1.12
S8	7481 ± 11	7435 ± 27	0.61
S9	8938 ± 6	8918 ± 22	0.23
S10	8082 ± 22	8063 ± 60	0.23
S13	7627 ± 23	7629 ± 57	0.03

Static and Dynamic Permittivity Measurement of High Explosives in the W Band to Investigate Shock and Detonation Phenomena

**Propellants,
Explosives,
Pyrotechnics**

from a transmission line system and a Nicholson Ross Weir modified method, yielding the complex permittivity; and (2) a dynamic approach based on the detonation wavefront tracking method using an interferometer operating at 94 GHz, yielding the real part of the relative permittivity. The latter uses the measurement of phase and Doppler frequency shift. The difference between relative permittivities given by these two approach is small and does not exceed 2 % for the real part. Losses for high explosives are measured in the W band and found to be low, in the order of 0.05–0.1 for non-aluminized high explosives. The inclusion of aluminum increases losses to the order 0.2–0.4. With the static results, the detonation velocity can be re-computed. These results are in very good agreement (deviation under 1 %) with shorting pins tracking. Both static and dynamic approaches are found here suitable for the measurement of the relative permittivity in the framework of detonation, shock wave studies and detection issue. Fourteen compositions are studied with various components, mass densities and inclusions. The addition of aluminum particle is well represented with the Bruggeman formula. The effect of the change in mass density is studied with various compositions and suggests that the Landau Lifschitz Looyenga model is the most adequate. Two almost identical composition but with a different grain morphology and a different mass density are studied. The Landau Lifschitz Looyenga model is still adequate but the deviation is larger than with other high explosives. The difference in the sizes of the grains is a proposed explanation for this deviation.

This works helps to develop a database of the permittivity of high explosives in the W band which could be useful for detection, microwave heating or front tracking applications.

Acknowledgements

References

[1] M. Chen, M. A. Zikry, M. B. Steer, Microwave Excitation of Crystalline Energetic Composites, *IEEE Access* **2018**, *6*, 24596.

[2] P. Smith, J. Weatherall, J. Barber, K. Yam, J. Greca, B. Smith, *Passive and Active Millimeterwave Imaging Technology XX*, Anaheim CA, USA, April, **2017**.

[3] D. Etayo, I. Maestrojuan, J. Teniente, I. Ederra, R. Gonzalo, Experimental Explosive Characterization for Counterterrorist Investigation, *J. Infrared Milli. Terahz. Waves* **2013**, *7–8*, 468.

[4] R. S. Janesheski, L. J. Groven, S. Son, Detonation failure characterization of non-ideal explosives, *AIP Conf. Proc.* **2012**, *1426*, 587.

[5] P. Rae, B. Glover, J. Gunderson, L. Perry, Free-field microwave interferometry for detonation front tracking and run-to-detonation measurements, *AIP Conf. Proc.* **2011**, *434*, 1426.

[6] J. Benterou, C. Bennett, G. Cole, D. Hare, C. May, E. Udd, *SPIE Defense*, *Security and Sensing*, Orlando FL, USA, **2009**.

[7] V. Belskii, A. Mikhailov, A. Rodionov, A. Sedov, Microwave Diagnostics of Shock-Wave and Detonation Processes, *Combust. Explos. Shock Waves* **2011**, *47*, 639.

[8] K. Chang, *Encyclopedia of RF and Microwave Engineering*, John Wiley & Sons, New York, **2005**.

[9] J. Barber, J. Weatherall, B. Smith, S. Duffy, S. Goettler, A. Krauss, *Passive and Active Millimeterwave Imaging Technology XIII* (Eds.: D. A. Wilkner, A. R. Luukanen), Orlando FL, USA, **2010**.

[10] G. Cawsey, J. Farrands, S. Thomas, Observations of Detonation in Solid Explosives by Microwave Interferometry, *Proc. R. Soc. Lond. A* **1958**, *248*, 499.

[11] M. E. Daily, B. Glover, S. Son, L. J. Groven, X-Band Microwave Properties and Ignition Predictions of Neat Explosives, *Propellants Explos. Pyrotech.* **2013**, *38*, 810.

[12] A. L. Higginbotham Duque, W. L. Perry, C. M. Anderson-Cook, Complex Microwave Permittivity of Secondary High Explosives, *Propellants Explos. Pyrotech.* **2014**, *39*, 275.

[13] B. B. Glover, W. L. Perry, Microwave Properties of TATB Particles from Measurements of the Effective Permittivity of TATB Powders, *Propellants Explos. Pyrotech.* **2009**, *34*, 347.

[14] J. Tringe, R. J. Kane, K. T. Lorenz, E. V. Baluyot, K. S. Vandersall, Dielectric characterization and microwave interferometry in HMX-based explosives, *J. Phys.: Conf. Ser.* **2014**, *500*, 142033.

[15] A. M. Nicholson, G. F. Ross, Measurement of the Intrinsic Properties of Materials by Time-Domain Techniques, *IEEE Trans. Instrum. Measurement* **1970**, *19*, 377.

[16] W. B. Weir, Automatic measurement of complex dielectric constant and permeability at microwave frequencies, *IEEE Proc.* **1974**, *62*, 33.

[17] T. Chang, X. Zhang, X. Zhang, H. Cui, Accurate determination of dielectric permittivity of polymers from 75 GHz to 1.6 THz using both S-parameters and transmission spectroscopy, *Appl. Optics* **2017**, *56*, 3287.

[18] D. E. Kittell, J. O. Mares Jr., S. F. Son, Using time-frequency analysis to determine time-resolved detonation velocity with microwave interferometry, *Rev. Sci. Instrum.* **2015**, *86*, 044705.

[19] V. Singh, A. R. Kulkarni, T. R. Rama Mohan, Dielectric properties of aluminum-epoxy composites, *J. Appl. Poly. Sci.* **2003**, *90*, 3602.

[20] K. Lal, R. Parshed, Permittivity of conductor-dielectric heterogeneous mixtures, *J. Phys. D: Appl. Phys.* **1973**, *6*, 1788.

[21] S. O. Nelson, Density-permittivity relationships for powdered and granular materials, *IEEE Trans. Instrum. Measurement* **2005**, *54*, 2033.

[22] K. N. Rozanov, A. V. Osipov, D. A. Petrov, S. N. Starostenko, E. P. Yelsukov, The effect of shape distribution of inclusions on the frequency dependence of permeability in composites, *J. Magnetism Magnetic Mater.* **2009**, *321*, 738.

[23] Joint Committee for Guides in Metrology, *Evaluation of measurement data – Guide to the expression of uncertainty in measurement*, JCGM 100:2008,120p, **2008**.